THE JOURNAL OF PHYSICAL CHEMISTRY B

 VOLUME 108, NUMBER 13, APRIL 1, 2004

LETTERS

Low Temperature Synthesis of Flowerlike ZnO Nanostructures by Cetyltrimethylammonium Bromide-Assisted Hydrothermal Process

Hui Zhang, Deren Yang,* Yujie Ji, Xiangyang Ma, Jin Xu, and Duanlin Que

State Key Lab of Silicon Materials, Zhejiang University, Hangzhou 310027, People's Republic of China

Received: September 21, 2003

The flowerlike ZnO nanostructures, which consisted of swordlike ZnO nanorods, have been prepared by a cetyltrimethylammonium bromide (CTAB)-assisted hydrothermal process at low temperature (120 °C). The XRD pattern indicated that the flowerlike ZnO nanostructures were hexagonal. Furthermore, the SAED and HRTEM revealed that the swordlike ZnO nanorods were single crystal in nature and preferentially grew up along [001]. Finally, the mechanism for the CTAB-assisted hydrothermal synthesis of flowerlike ZnO nanostructures has been preliminarily explained by polar crystal growth theory and surfactant action theory.

Introduction

Over the past decade, the synthesis and functionalization of nanostructures have attracted great interest due to their significant potential application.[1−3] Many kinds of semiconductor nanowires and nanotubes such as Si, GaN, CdS, Se, etc. have been prepared.[4−7] Other interesting one-dimensional nanostructures including nanobelts, nanoribbons, and nanocable have also been fabricated.[8−10] Semiconductor oxide nanomaterials, such as ZnO, Ga_2O_3, In_2O_3, and SnO_2, have been hot subjects because of the wide use as basic materials for transparent conducting films, photoelectronics, and gas sensors.[11−14] Among them, ZnO is of interest for low-voltage and short wavelength electrooptical devices such as light emitting diodes and diode lasers due to its wide band gap (3.2 eV) and large exciton binding energy of 60 meV.[15] Many interesting nanostructures of ZnO including nanobelts, nanobridges, nanonails, and nanoribbons have been fabricated by thermal evaporation of oxide powders.[16−19] Recently, the synthesis of ZnO nanowires and nanorods by a solvothermal process has also been reported.[20,21] However, it is inevitable to use toxic, dangerous, and expensive solvents such as amine in solvothermal process. As for ZnO nanorods, it is also necessary to prepare them at a high temperature of more than 160 °C. Very recently, cetyltrimethylammonium bromide (CTAB, a cationic surfactant) was used to prepare PbO nanorods.[22] Herein, we prepared flowerlike single-crystal ZnO nanostructures by the CTAB-assisted hydrothermal process at low temperature (120 °C). Moreover, the mechanism for the CTAB-assisted hydrothermal synthesis of flowerlike ZnO has been preliminary presented.

Experimental Section

All the chemicals were analytic grade reagents without further purification. Experimental details were as follows: 0.5 g of $Zn(AC)_2$ was put into 110 mL of saturated CTAB aqueous solution under stirring. After 10 min stirring, 10 mL of 2 M NaOH aqueous solution was introduced into the aqueous solution under stirring, resulting in a white aqueous solution, which was then transferred into Teflon-lined stainless steel autoclaves, sealed, and maintained at 120 °C for 20 h. For the comparison, two similar other experiments were performed. One was without CTAB; the other was at 160 °C. And then, the resulting white solid products were centrifuged, washed with distilled water and ethanol to remove the ions possibly remaining in the final products, and finally dried at 60 °C in air.

The obtained samples were characterized by X-ray powder diffraction (XRD) using a Rigaku D/max-ga X-ray diffrac-

* Corresponding author. mseyang@dial.zju.edu.cn.

10.1021/jp036826f CCC: $27.50
Published on Web 03/10/2004

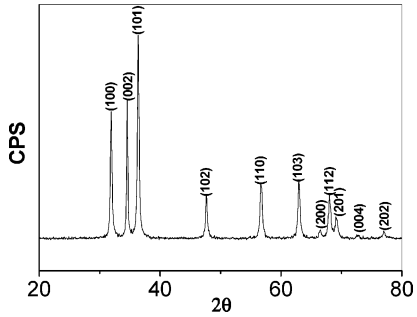

Figure 1. XRD pattern of the flowerlike ZnO nanostructures prepared by the CTAB-assisted hydrothermal process at the low temperature (120 °C).

tometer with graphite monochromatized and Cu Ka radiation (λ = 1.541 78 Å). The scanning electron microscopy images were obtained on JSM-T20. Transmission electron microscopy (TEM) observation was performed with a Philips CM 200 microscope operated at 200 kV.

Results and Discussion

The XRD pattern of the flowerlike ZnO nanostructures prepared by CTAB-assisted hydrothermal method is shown in Figure 1. All the diffraction peaks can be indexed as the hexagonal ZnO with lattice constants $a = 3.249$ and $c = 5.206$ Å, which are consistent with the values in the standard card (JCPDS 36-1451). Compared to the standard card, the (002) peak is stronger, revealing the [001] oriented growth of the ZnO nanorods. Even if fabricated at the low temperature, the flowerlike ZnO nanostructures crystallized well, according to the intensity and half width of the XRD pattern.

Figure 2a shows the SEM image of flowerlike ZnO nanostructures. The typical flowerlike ZnO nanostructures consisted of the ZnO swordlike nanorods with 60−200 nm in width and several micrometers in length, as shown in Figure 2b. The definition of the flowerlike ZnO nanostructures comes from the geometrical similarity to flowers. In our experiments, it is impossible that the aggregation resulted in the flowerlike nanostructures, because long time ultrasonic treatment could not destroy the nanostructures.

Figure 3a shows the TEM image of an individual ZnO nanorod obtained from the flowerlike ZnO nanostructures treated by long time ultrasonic. From this image, it can be seen that an end of the ZnO nanorod is pointed like a sword. The selected area electron diffraction (SAED) pattern inserted in Figure 3a indicates that the nanorod is of single crystal and can be indexed as the hexagonal ZnO phase, which is in accord with the XRD results in Figure 1, implying that the flowerlike ZnO nanostructures consisting of swordlike ZnO nanorods are hexagonal phase single crystal. Figure 3b shows the typical high-resolution transmission electron microscopy (HRTEM) image of the individual swordlike ZnO nanorod shown in Figure 3a. The

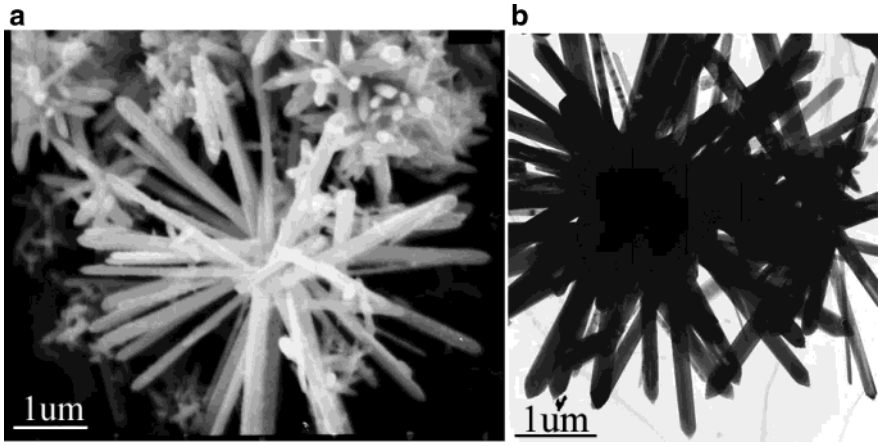

Figure 2. SEM image (a) and TEM image (b) of the flowerlike ZnO nanostructures by CTAB-assisted hydrothermal process at the low temperature (120 °C).

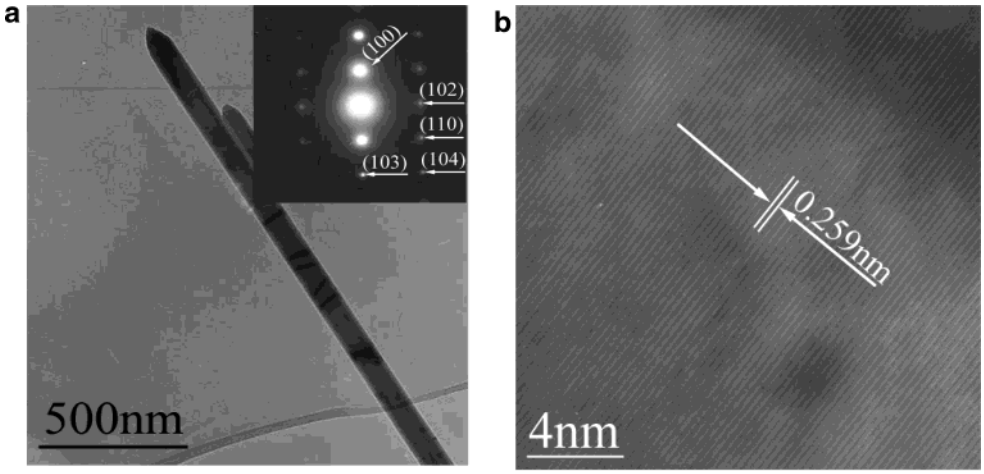

Figure 3. TEM image (a) and HRTEM image (b) of an individual swordlike ZnO nanorod, which composes the flowerlike ZnO nanostructures by the CTAB-assisted hydrothermal process at the low temperature (120 °C). The upper right inset in (a) corresponds to the SAED pattern of the relative swordlike ZnO nanorod.

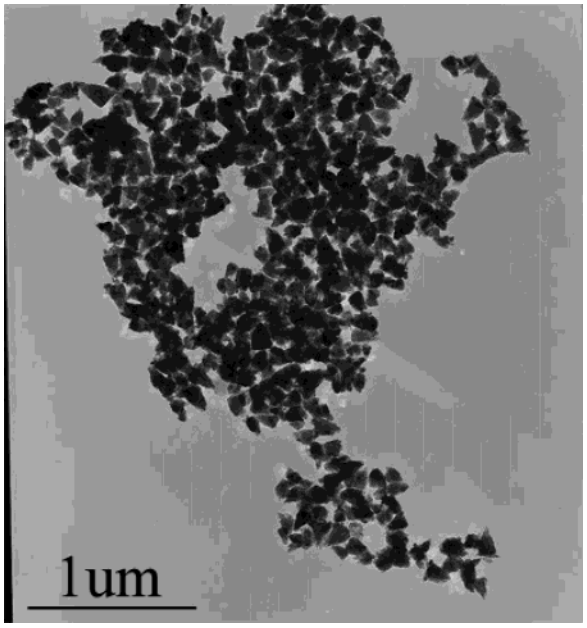

Figure 4. TEM image of the ZnO nanoparticles prepared by the hydrothermal process without CTAB at the low temperature (120 °C).

image clearly reveals only the fringes of (002) planes with a lattice spacing of about 0.259 nm can be observed, indicating that the ZnO nanorod is single crystal in nature, which is in according with the SAED pattern inserted in Figure 3a. Furthermore, the spacing of 0.259 nm between adjacent lattice planes corresponds to the distance of (002) planes, indicating that [001] is the growth direction of the ZnO nanorods.

To substantially understand the effect of CTAB on the flowerlike ZnO nanostructures, the experiments of hydrothermal process without CTAB were carried out. Figure 4 shows the TEM image of the ZnO nanoparticles prepared by the hydrothermal process without CTAB. The size of the ZnO nanoparticles is about 100 nm, similar to that of the swordlike ZnO nanorods. The ends of the ZnO nanoparticles are also pointed. The reason, in this experiment, swordlike ZnO nanorods did not grow at the low temperature (120 °C) was that without CTAB there were not enough driving force.

In general, a larger ZnO crystal is a polar crystal whose positive polar plane is rich in Zn and the negative polar plane is rich in O. In the hydrothermal process, the growth unit of ZnO is $[Zn(OH)_4]^{2-}$, which leads to the different growth rate of planes shown in following: $V_{(0001)} > V_{(\bar{1}01\bar{1})} > V_{(\bar{1}010)} > V_{(\bar{1}011)} > V_{(000\bar{1})}$. As we know, the more rapid the growth rate, the quicker the disappearance of the plane. Therefore, the (0001) plane, the most rapid growth rate plane, disappears in the hydrothermal process, which leads to the pointed shape in an end of the *c* axis, shown in Figure 5a.[23,24] However, the $(000\bar{1})$ plane, the slowest growth rate plane, is maintained in the hydrothermal process, which leads to the plain shape in another end of the *c* axis. In fact, the growth mechanism of the flowerlike ZnO nanostructures is similar to that of larger ZnO crystals, as displayed in Figure 5b. In the experiments, OH^- is first introduced into Zn^{2+} aqueous solution, and then $Zn(OH)_2$ colloids form, according to

$$Zn^{2+} + 2OH^- \leftrightarrow Zn(OH)_2 \quad (1)$$

If the pH value in the aqueous solution is about 11, $Zn(OH)_2$ is the main composition. During the hydrothermal process, part of the $Zn(OH)_2$ colloids dissolves into Zn^{2+} and OH^- according to reaction 2. When the concentration of Zn^{2+} and OH^- reaches the supersaturation degree of ZnO, ZnO nuclei will form according to reaction 3. Thus, the growth units of $[Zn(OH)_4]^{2-}$ form according to reaction 4:

$$Zn(OH)_2 \rightarrow Zn^{2+} + 2OH^- \quad (2)$$

$$Zn^{2+} + 2OH^- \leftrightarrow ZnO + H_2O \quad (3)$$

$$Zn(OH)_2 + 2OH^- \leftrightarrow [Zn(OH)_4]^{2-} \quad (4)$$

Cheon et al. reported that there are four different parameters, kinetic energy barrier, temperature, time, and capping molecules, that can influence the growth pattern of nanocrystals under nonequilibrium kinetic growth conditions in the solution-based approach.[25] In our experiments, the temperature and capping molecules are the key parameters. In the hydrothermal process without CTAB, there are no active sites around the circumference of ZnO nuclei. Furthermore, the growth rate of the *c* axis is slow because the reaction temperature is low. Consequently, ZnO nanoparticles are obtained (Figure 4 and Figure 5b(1)). However, in the CTAB-assisted hydrothermal process, due to

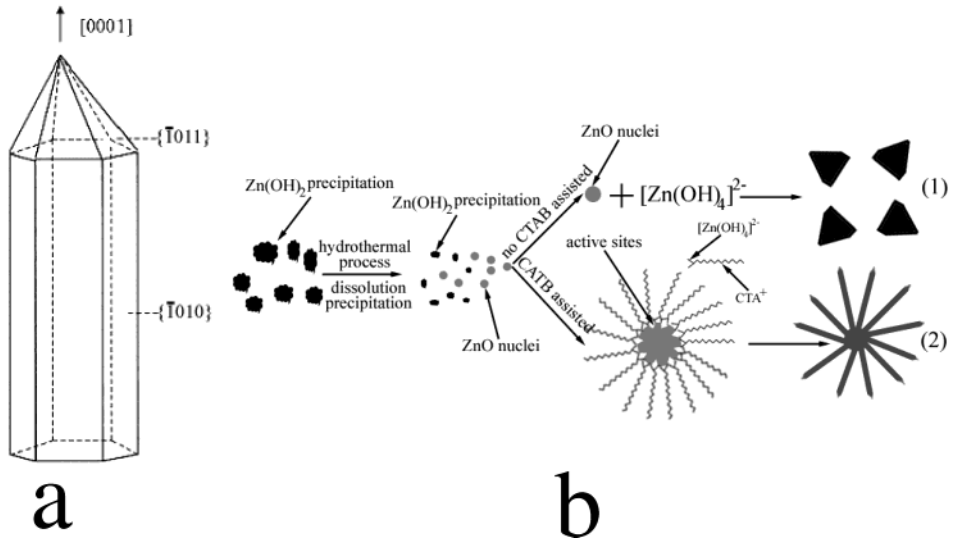

Figure 5. (a) Growth sketch of larger ZnO crystal. (b) Growth schematic diagram of ZnO nanostructures by the hydrothermal process at the low temperature (120 °C) with and without CTAB.

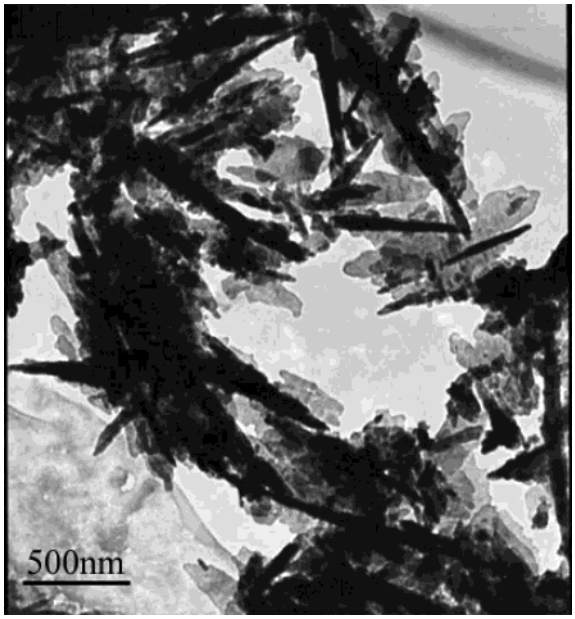

Figure 6. TEM image of the needlelike ZnO nanostructures prepared by the CTAB-assisted hydrothermal process at the relative high temperature (160 °C).

the surfactant, capsules of CTAB are generated in the saturation solution. Moreover, due to the coulomb force action between $[Zn(OH)_4]^{2-}$ and CTAB capsules, which are cation surfactants, they interact to form complexing agents, which are adsorbed on the circumference of the ZnO nuclei (Figure 5b(2)). Because of the adsorption of the complexing agents, the surface energy of ZnO nuclei decreases, resulting in the active sites generating on the surface. Thus, even if at the low temperature (120 °C), ZnO nanorods with pointed ends can grow on those active sites.

To confirm the effect of CTAB on the flowerlike ZnO nanostructures, the CTAB-assisted hydrothermal process at 160 °C was performed. Figure 6 shows the TEM image of the prepared ZnO nanostructures. It clearly indicates that only needlelike ZnO nanorods, but not flowerlike ZnO nanostructures, are obtained. Normally, the capsules of CTAB are destroyed at 160 °C in the hydrothermal process. Therefore, only an individual CTAB molecule interacts with $[Zn(OH)_4]^{2-}$ to form a complexing agent. Once this agent adsorbs on the surface of ZnO nuclei, an active site will form so that needlelike ZnO preferentially grows on this site.

In summary, flowerlike ZnO nanostructures, which consisted of swordlike ZnO nanorods, have been prepared by the CTAB-assisted hydrothermal process at a low temperature (120 °C). The flowerlike ZnO nanostructures are hexagonal phase and single crystal in nature. It is considered that CTAB can interact with growth units of ZnO to generate active sites on the surface of ZnO nuclei so that swordlike ZnO nanorods are created on those sites, resulting in the formation of the flowerlike ZnO nanostructures.

Acknowledgment. We appreciate the financial supports of the Natural Science Foundation of China (No. 60225010) and the Zhejiang Provincial Natural Science Foundation of China (No. 601092).

References and Notes

(1) Duan, X.; Huang, Y.; Agarwal, R.; Lieber, C. M. *Nature* **2003**, *421*, 241.
(2) Fuhrer, M. S.; Nygard, J.; Shih, L.; Forero, M.; Yoon, Y. G.; Mazzoni, M. S. C.; Choi, H. J. *Science* **2000**, *288*, 494.
(3) Ren, Z. F.; Huang, Z. P.; Xu, J. W.; Wang, J. H.; Bush, P.; Siegal, M. P.; Provencio, P. N. *Science* **1998**, *282*, 1105.
(4) Morales, A. M.; Lieber, C. M. *Science* **1998**, *279*, 208.
(5) Han, W. Q.; Fan, S. S.; Li, Q. Q.; Hu, Y. D. *Science* **1997**, *277*, 1287.
(6) Zhang, H.; Ma, X. Y.; Xu, J.; Niu, J. J.; Sha, J.; Yang, D. R. *J. Cryst. Growth* **2002**, *246*, 208.
(7) Hui Zhang, Xiangyang Ma, Yujie Ji, Jin Xu, Deren Yang, *Chem. Phys. Lett.* **2003**, *377*, 654.
(8) Mo, M. S.; Zeng, J. H.; Liu, X. M.; Yu, W. C.; Zhang, S. Y.; Qian, Y. T. *Adv. Mater.* **2002**, *14* (22), 1658.
(9) Liu, Z. P.; Peng, S.; Xie, Q.; Hu, Z. K.; Yang, Y.; Zhang, S. Y.; Qian, Y. T. *Adv. Mater.* **2003**, *15* (11), 936.
(10) Wang, X. D.; Gao, P. X.; Li, J.; Summers, C. J.; Wang, Z. L. *Adv. Mater.* **2003**, *14* (23), 1732.
(11) Ginley, D. S.; Bright, C. *Mater. Res. Bull.* **2000**, *25*, 15.
(12) Sberveglieri, G. et al. *Sens. Actuators B* **1995**, *25*, 588.
(13) Aoki, T.; Hatanaka, Y.; Look, D. C. *Appl. Phys. Lett.* **2000**, *76*, 3257.
(14) Ohta, H. et al. *Appl. Phys. Lett.* **2000** *77*, 475.
(15) Wong, E. M.; Searson, P. C. *Appl. Phys. Lett.* **1999**, *74*, 2939.
(16) Pan, Z. W.; Dai, Z. R.; Wang, Z. L. *Science* **2001**, *291*, 1947.
(17) Lao, J. Y.; Huang, J. Y.; Wang, D. Z.; Ren, Z. F. *Nano Lett.* **2003**, *3* (2), 235.
(18) Lao, J. Y.; Huang, J. Y.; Wang, D. Z.; Ren, Z. F. *Nano Lett.* **2002**, *2* (11), 1287.
(19) Ye, C.; Meng, G.; Wang, Y.; Jiang, Z.; Zhang, L. *J. Phys. Chem. B* **2002**, *106*, 10338.
(20) Zhang, J.; Sun, L. D.; Pan, H. Y.; Liao, C. S.; Yan, C. H. *New J. Chem.* **2002**, *26*, 33.
(21) Pacholski, C.; Kornowski, A.; Weller, H.; *Angew. Chem., Int. Ed.* **2002**, *41* (7), 1188.
(22) Cao, M. H.; Hu, C. W.; Peng, G.; Qi, Y. J.; Wang, E. B. *J. Am. Chem. Soc.* **2003**, *125*, 4982.
(23) Lioudmila N. D.; Dmitriy V. K. *Ann. Chim. Sci. Mat,* **2001**, *26*, 193.
(24) Li, W. J.; Shi, E. W.; Zhong, W. Z.; Yin, Z. W. *J. Synth. Cryst.* **1999**, *28* (2), 117.
(25) Lee, S. M.; Cho, S. N.; Cheon, J. W. *Adv. Mater.* **2003**, *15* (5), 441.